Synaptic Dysfunction and Compensation After NMDA Receptor Ablation in the Mouse Medial Prefrontal Cortex

Rachel M. Dick[1], Lydia B. Cunitz[2], Aurora Torres Pérez[3], Habsa Ahmed[2], Anisha P. Adke[4], Cristina Rivera Quiles[2], Jason S. Mitchell[5], Ezequiel Marron Fernandez de Velasco[6], Nicola M. Grissom[7] & Patrick E. Rothwell[2*]

[1]Graduate Program in Neuroscience, University of Minnesota, Minneapolis, MN

[2]Department of Neuroscience, University of Minnesota, Minneapolis, MN

[3]University of Puerto Rico - Río Piedras, San Juan, PR

[4]Medical Scientist Training Program, University of Minnesota, Minneapolis, MN

[5]Department of Microbiology and Immunology, University of Minnesota, Minneapolis, MN

[6]Department of Pharmacology, University of Minnesota, Minneapolis, MN

[7]Department of Psychology, University of Minnesota, Minneapolis, MN

*Corresponding Author:

Patrick E. Rothwell, Ph.D.
4-142 Wallin Medical Biosciences Building
2101 6th Street SE
Minneapolis, MN, 55455
Phone: 612-626-8744
Email: rothwell@umn.edu

ABSTRACT

N-methyl-D-aspartate receptors (NMDARs) in the prefrontal cortex (PFC) are critical regulators of neuronal excitability, synaptic plasticity, and cognitive function. NMDAR disruptions, including pharmacological blockade and anti-NMDAR encephalitis, can mimic symptoms of schizophrenia. These observations support the glutamate hypothesis of schizophrenia, which posits that symptoms arise from abnormal corticolimbic glutamatergic signaling. Further evidence for this theory includes abnormal expression of NMDARs and decreased dendritic spine density in the PFC of individuals with schizophrenia, as well as altered spine density and synaptic transmission caused by genetic manipulation of NMDARs. However, it is unknown how progressive loss of NMDAR function in the PFC during adolescence – a developmental time period associated with significant synaptic pruning and symptom onset in schizophrenia – affects excitatory synaptic structure and function. In this study, we used in vivo genome editing to ablate expression of the Grin1 gene, which encodes the obligate GluN1 subunit of NMDARs, in medial PFC neurons of female and male adolescent mice. We assessed synaptic density and function in layer V pyramidal neurons at multiple time points using whole-cell patch-clamp electrophysiology, integrated with confocal imaging of dendritic spine architecture in recorded neurons. NMDAR ablation caused an early decrease in basilar dendritic spine density, followed by a rebound in spine density and corresponding increase in AMPAR-mediated synaptic transmission, suggesting that synaptic compensation maintains an allostatic set point. Our findings demonstrate that NMDAR ablation initially disrupts local PFC networks, followed by recovery via compensatory processes that could be impaired in disease states.

INTRODUCTION

Abnormal glutamatergic signaling in the prefrontal cortex (PFC) is one of several biomarkers associated with schizophrenia [1]. Convergent evidence from genome-wide association studies [2,3], postmortem tissue histology [4,5], and in vivo neuroimaging [6,7] indicating altered expression and function of N-methyl-D-aspartate receptors (NMDARs). Early evidence for the link between glutamatergic signaling and schizophrenia came from studies showing that the administration of NMDAR antagonists such as phencyclidine (PCP) and ketamine induces a psychotomimetic state in healthy individuals [8,9] and worsen symptoms in patients [10–12]. Repeated NMDAR administration in rodents and primates also leads to cognitive deficits and progressive decreases in the synchronous firing of PFC neurons, which may be related to loss of synaptic connectivity [13–17]. This is consistent with human postmortem tissue studies demonstrating a reduction in dendritic spine density in patients with schizophrenia, specifically in the basilar dendrites of deep layer III neurons in the dorsolateral PFC [18,19]. These deficits in neural synchrony and spine architecture support the theory of activity-dependent disconnection [20–23], which posits that NMDAR loss drives spike timing defects in neurons and leads to subsequent weakening of PFC circuits [24].

NMDARs are heterotetrameric proteins containing two obligatory GluN1 subunits encoded by the Grin1 gene and two GluN2 and/or GluN3 subunits [25]. Although Grin1 mutations are not strongly associated with schizophrenia, manipulation of the Grin1 gene has served as a longstanding model for understanding the effects of decreased glutamatergic signaling. Initial research on the impact of NMDAR ablation upon neuroanatomy and physiology was conducted using mice with a homozygous genetic knockout of Grin1, which prevents the assembly of functional NMDARs [26]. However, *Grin1*$^{-/-}$ mice die 8-15 hours after birth due to respiratory failure, making them an unsuitable model for studying the long-term effects of NMDAR hypofunction [27]. The lethal effect of full Grin1 knockout can be avoided by using a more targeted approach; for instance, sparse Grin1 deletion in cultured cells or region-specific knockout in vivo. The impacts of these manipulations differ substantially depending on the brain region, developmental window, and method. Global

knockdown of Grin1 to 10% of normal levels leads to reduced dendritic spine density in striatal medium spiny neurons [28] and unstable spines and reduced spine density in organotypic hippocampal slices [29]. In contrast, spiny stellate cells in layer IV of the barrel cortex have increased spine density in a cortical Grin1 knockout mouse [30].

These structural changes in dendritic spine architecture can also be associated with complex changes in excitatory synaptic transmission. Conditional genetic knockout of Grin1 in cortex and hippocampus with Nex-Cre mice leads to decreased spine density and a shortened lifespan of less than one month, but increased AMPAR-mediated synaptic transmission due to greater presynaptic axon bouton volume and postsynaptic density area [31]. Sparse conditional knockout of Grin1 in cultured hippocampal neurons also increases AMPAR-mediated synaptic transmission, but with no corresponding change in dendritic spine density [32]. This study also indicates that the timing of NMDAR manipulation may dictate functional consequences, as there was no change in AMPAR-mediated synaptic transmission when Grin1 was deleted in the hippocampus of mature mice (>P60). This temporal window for efficacy of NMDAR manipulation may vary between brain regions, as the effects of Grin1 deficiency on excitatory synaptic function in the mouse medial PFC (mPFC) can be rescued by restoring NMDAR expression in adulthood [33], indicating that the mature mPFC retains some of its capacity for neuroplasticity.

Taken together, the prior literature provides evidence that reduction of NMDAR function leads to changes in spine density and excitatory synaptic transmission, yet there is a critical lack of knowledge regarding the effects of NMDAR manipulation in the frontal cortex during adolescence. This is a relevant developmental period characterized by significant synaptic pruning [34] and the beginning of symptom onset in schizophrenia [35–39]. Adolescent manipulation of NMDAR function may also be relevant to anti-NMDAR encephalitis, which frequently develops during adolescence and produces symptoms that resemble acute psychosis [40,41]. To address these issues, we leveraged recent advances in genome editing that have made it possible to perform localized and chronic genetic manipulations in the mature nervous system in vivo [42,43]. We utilized clustered regularly interspaced short palindromic repeats (CRISPR)-Cas9 technology to delete the

50 Grin1 gene encoding the obligate GluN1 subunit of NMDARs in mouse mPFC, and examined the effects of
51 progressive loss of NMDAR function upon synaptic reorganization, by measuring synaptic strength and
52 density at multiple time points during adolescence and early adulthood. We integrated electrophysiological
53 measurements with confocal imaging of dendritic spines in order to understand how complex interrelated
54 changes in neurotransmission and synaptic architecture may unfold over time in response to the loss of
55 NMDARs.
56
57 **MATERIALS & METHODS**
58 **Animals**
59 Mice expressing a Cre-dependent Cas9-GFP transgene [44] were maintained on a C57Bl/6J genetic
60 background. All experimental procedures were approved by the Institutional Animal Care and Use Committee
61 at the University of Minnesota, and observed the NIH Guidelines for the Care and Use of Laboratory Animals.
62 For additional details, see Supplementary Information.
63
64 **Surgical procedures**
65 As previously described [45], mice between 5-6 weeks old underwent intracranial viral injections.
66 Virus was infused bilaterally (500 nL each side at 120 nL/min) into the mPFC (AP: +1.80 mm, ML: ±0.35
67 mm, DV: −2.2 mm from bregma). Data were collected two weeks (14-27 days), four weeks (28-41 days), or
68 six weeks (42-55 days) post-surgery. For additional details, see Supplementary Information.
69
70 **Immunohistochemistry for virus expression**
71 Mice were deeply anesthetized using sodium pentobarbital (Fatal-Plus, Vortech Pharmaceuticals) and
72 transcardially perfused with ice cold 0.01 M PBS followed by ice cold 4% PFA in 0.01 M PBS. Brains were
73 extracted and post-fixed in 4% PFA at 4ºC overnight, then transferred to a 10% sucrose solution. Following
74 sectioning and immunohistochemistry, slices were mounted in PBS and coverslipped onto glass slides using

ProLong Diamond Antifade mountant (Thermo Fisher Scientific). For additional details, see Supplementary Information.

Brain slice electrophysiology

Coronal sections containing mPFC were collected as previously described [46]. Whole-cell voltage-clamp recordings were conducted in virally transduced pyramidal neurons in mPFC layer V. For additional details, see Supplementary Information.

Confocal imaging and analysis of dendritic spines

Following whole-cell patch-clamp recordings with internal pipette solution containing neurobiotin, the pipette was slowly retracted until a gigaohm seal was formed, indicating successful separation from the membrane of the recorded cell that was preserved for morphological analysis. Dendritic spines were imaged using a Leica Stellaris 8 confocal microscope operated by a workstation running Leica LAS X acquisition software (version 4.6.1). All spine data was analyzed using Bitplane Imaris software (version 10.1). For additional details, see Supplementary Information.

Statistical analysis

Similar numbers of male and female animals were used in all experiments, with sample sizes indicated in figure legends (n = number of cells, N = number of animals) and illustrated by individual data points in figures, with a visual distinction between cells from females (open circles) and males (filled circles). Sex was included as a variable in factorial ANOVA models analyzed using GraphPad Prism version 10, with repeated measures on within-subject factors. Significant ANOVA interactions were decomposed by analyzing simple effects (i.e., the effect of one variable at each level of the other variable). Significant main effects were analyzed using Fisher's Least Significant Difference (LSD) post-hoc tests. The Type I error rate was set to $\alpha = 0.05$

99 (two-tailed) for all comparisons. All summary data are displayed as mean +/- SEM. All figures were created
100 in BioRender.
101
102 **RESULTS**
103 **Validation of NMDAR Ablation using in vivo Genome Editing**
104 To eliminate NMDAR expression, we used transgenic male and female mice expressing Cas9 and
105 eGFP from the Rosa26 locus in a Cre-dependent fashion [44]. To activate Cas9 expression in mPFC neurons,
106 we performed bilateral stereotaxic injection of an adeno-associated virus (AAV), with expression of mCherry-
107 Cre driven by the human synapsin (hSyn) promoter sequence. The same AAV vector also expressed a guide
108 RNA targeting the Grin1 gene [47], which encodes the obligate GluN1 subunit of NMDARs (Fig 1A). As a
109 control, separate groups of mice were injected with a virus expressing a guide RNA for LacZ (a bacterial gene
110 not present in mammals) in place of the Grin1 guide RNA. Stereotaxic injection of these AAV vectors was
111 performed in adolescent mice at 5-6 weeks of age, a time point selected to mirror a developmental period
112 associated with significant pruning of cortical networks [48,49] and the onset of schizophrenia-related
113 symptoms in some patients [50]. We confirmed viral expression in the mPFC based on mCherry fluorescence,
114 with co-localized GFP fluorescence by individual neurons indicating Cre-mediated transgene expression (Fig
115 1B).
116 To confirm successful ablation of the Grin1 gene and subsequent loss of NMDAR function in virally
117 transduced cells, we performed whole-cell patch-clamp recordings from layer V pyramidal neurons in acute
118 mPFC brain slices, prepared 2-6 weeks after stereotaxic surgery. NMDAR current was measured by recording
119 electrically-evoked excitatory postsynaptic currents (EPSCs) at +40 mV and calculating the amplitude at 50
120 ms post-stimulus, by which point much of the fast AMPAR current has decayed (Fig. 1C) [51]. AMPAR
121 current was measured by recording EPSCs at -70 mV and calculating the peak amplitude. At all timepoints,
122 there was a significant reduction in the NMDAR/AMPAR ratio in the Grin1 group compared to the control
123 group (Fig 1D). The half-width of the dual component EPSC (NMDAR+AMPAR) recorded at +40 mV was

124 similarly reduced at all timepoints (Fig 1E). This indicates that the change in the NMDAR/AMPAR ratio is
125 due to a loss of NMDARs, which have slower kinetics and therefore produce a more sustained excitatory
126 current at +40 mV compared to AMPARs. After six weeks of Grin1 virus expression, decreases in average
127 NMDAR/AMPAR ratio and dual EPSC half-width were comparable to pharmacological blockade of NMDAR
128 function with 50 μM D-APV (dotted line in Fig 1D-E), indicating robust loss of NMDAR function.
129

130 **Dendritic Spine Architecture after NMDAR Ablation**

131 To quantify synaptic density after ablation of NMDAR expression, we filled individual neurons with
132 neurobiotin during whole-cell patch-clamp recordings, and then performed confocal imaging of dendritic
133 architecture in the same pyramidal neurons (Fig 2A). Using Imaris software, spines were also automatically
134 classified into four morphological groups: mushroom spines, which tend to be more stable and associated with
135 greater synaptic strength; and filopodia/dendrites, stubby spines, and long/thin spines, which are more
136 immature and weaker [52].

137 In the basilar dendritic arbor (Fig 2B-C), we observed differences between the Grin1 and control groups
138 that varied across time. At 2 weeks, there is a significant decrease in basilar spines in the Grin1 group (Fig
139 2D), with a corresponding leftward shift in the cumulative probability distribution (Fig 2E), driven primarily
140 by a loss of thin spines and filopodia (Fig 2H). This same trend was observed to a lesser extent at 4 weeks (Fig
141 2F), with a significant decrease in the densities of mushroom spines (Fig. 2I). At six weeks, this pattern
142 reversed (Fig. 2D) and the cumulative probability distribution shifted rightward toward a significant *increase*
143 in the Grin1 group compared to LacZ (Fig 2G), a pattern most apparent in the less mature spine categories
144 (Fig. 2J). These morphological changes were specifically observed in the basilar dendritic arbor, as no
145 significant changes in total spine density or specific spine categories were observed at any time point in the
146 apical dendritic arbor of the same cells (Fig. S1).
147

148 **Functional Correlates of Synaptic Strength and Density**

149 To investigate the functional implications of these alterations in synaptic architecture, we recorded
150 miniature excitatory postsynaptic currents (mEPSCs) in the presence of tetrodotoxin (500 nM), providing a
151 measure of spontaneous excitatory neurotransmission (Fig 3A). The mEPSC amplitude, which is a correlate
152 of postsynaptic strength, was not significantly changed at any time point (Fig 3B). However, there was a
153 significant increase in mEPSC frequency at 6 weeks (Fig 3C), with a corresponding leftward shift in the
154 cumulative probability distribution of mEPSC inter-event intervals at 4 and 6 weeks (Fig 3F and 3H), but not
155 at 2 weeks (Fig 3D).

156 We also evaluated potential changes in mEPSC frequency as a function of event size. mEPSC
157 amplitude can be influenced by synaptic location – i.e., events that originate at more distal synapses tend to
158 have a smaller amplitude due to dendritic filtering, whereas events that originate closer to the soma tend to be
159 larger [53]. At all timepoints, the relative difference in mEPSC frequency between Grin1 and control groups
160 was similar, regardless of amplitude (Fig 3E, 3G, 3I).

161 To determine whether changes in spine density and excitatory synaptic transmission were caused by a
162 cell-autonomous effect in pyramidal neurons, we used the same CRISPR-Cas9 genome editing strategy, but
163 replaced the hSyn promoter sequence of our viral vectors with the CaMKII promoter sequence (Fig S2A). The
164 efficacy of this manipulation was confirmed by a significant decrease in the NMDAR/AMPAR ratio 2 weeks
165 after virus injection (Fig S2B-D). However, we did not observe significant changes in basilar spine density at
166 this time point (Fig S2E-H). There were also no changes in mEPSC amplitude or frequency at any time point
167 after Grin1 ablation using the CaMKII promoter (Fig S3), suggesting loss of NMDAR function from pyramidal
168 neurons is not sufficient to cause the effects observed using the hSyn promoter.

169

170 **Compensatory Changes in Synaptic Transmission**

171 Taken together, the changes in synaptic structure and function described above point towards an initial
172 loss of dendritic spines in the Grin1 group. This is followed by a recovery of dendritic spine density that returns
173 to and overshoots control levels, with a corresponding increase in mEPSC frequency. These changes may
174 emerge as a compensatory response to the ablation of NMDARs, so we next investigated other potential
175 compensatory changes in excitatory or inhibitory synaptic transmission. Following six weeks of virus
176 expression, there was no change in the paired-pulse ratio of evoked EPSCs at interstimulus intervals ranging
177 from 25-400 ms (Fig 4A-B). This indicates that presynaptic glutamate release probability was unaffected by
178 NMDAR ablation, and also suggests the increase in mEPSC frequency at the same time point was related to
179 dendritic spine density and synapse number, rather than a change in the probability of glutamate release.

180 We next examined the possibility that NMDAR ablation and corresponding loss of calcium influx could
181 lead to compensatory changes in AMPAR subunit composition, such as increased contribution of AMPARs
182 lacking the GluA2 subunit [54,55]. Subunit composition can influence the kinetic properties of AMPAR
183 currents, but there was no change at any time point in the half-width of the isolated AMPAR current recorded
184 at -70 mV as part of the NMDAR/AMPAR ratio measurement (Fig 4C). Calcium-permeable AMPARs lacking
185 a GluA2 subunit are blocked by intracellular polyamines at depolarized membrane potentials, producing a non-
186 linear current-voltage relationship. However, following six weeks of virus expression, there was no difference
187 in the AMPAR current-voltage relationship (Fig 4D-E), and no change in the rectification index comparing
188 current passed at depolarized versus hyperpolarized membrane potentials (Fig. 4F). These data suggest that
189 the subunit composition of AMPARs does not change following NMDAR ablation.

190 Given the increase in dendritic spine density and mEPSC frequency following six weeks of virus
191 expression, we also explored potential adaptations at the level of inhibitory synaptic transmission, by recording
192 miniature inhibitory postsynaptic currents (mIPSCs) at this time point (Fig 5A). Following six weeks of virus
193 expression, we observed a significant increase in average mIPSC amplitude (Fig 5B-C), but no change in

194 mIPSC frequency (Fig 5D-E). These results suggest that following protracted NMDAR ablation, the overall
195 excitatory-inhibitory balance of the mPFC network may be maintained by stabilizing at a new allostatic set
196 point (Fig. 5F-G).
197
198 **DISCUSSION**
199 Our findings reveal significant time-dependent structural and functional reorganization of cortical
200 networks following NMDAR manipulation during adolescence. We observed a change in basilar spine density
201 as NMDAR ablation progressed, with initial spine loss in the Grin1 group at earlier time points shifting towards
202 an increase in spine density at 6 weeks. This effect was primarily driven by thin spines, which are associated
203 with weaker synapses and appear or disappear in response to synaptic activity [56], as well as filopodia, which
204 have a short lifespan and may not form functional synapses due to their lack of postsynaptic density [52]. This
205 is consistent with evidence from human postmortem tissue studies showing a selective loss of smaller spines
206 in the cortex of patients with schizophrenia [57,58]. We did not observe a change in apical spine density at
207 any time point. This suggests that the local mPFC microcircuitry may be more vulnerable to the effects of
208 NMDAR ablation, since basilar dendrites receive inputs from other nearby neurons, whereas apical dendrites
209 receive more long-range cortical and thalamic signals [59]. This basilar-specific effect is consistent with
210 evidence of decreased synchronous firing between pairs of prefrontal neurons following NMDAR blockade
211 [16], which indicates that disruption of local PFC connections may be a key consequence of NMDAR
212 hypofunction.
213 We were surprised that changes in dendritic spine architecture were observed in the basilar but not the
214 apical dendritic arbor of layer V pyramidal neurons. Studies of postmortem tissue from patients with
215 schizophrenia have documented a reduction in dendritic spine density in the basilar dendrites of deep layer III
216 neurons in the dorsolateral PFC (dlPFC). Based on these previous studies, it has been suggested that apical
217 dendrites in layer V neurons may be vulnerable to spine loss in schizophrenia, since deep layer apical dendrites

218 and superficial layer basilar dendrites both receive inputs from the mediodorsal nucleus of the thalamus within
219 layer III [60]. In contrast, the significant increase in basilar spine density that we observed at 6 weeks suggests
220 that the network is overcompensating for early initial spine loss. This may be attributed to the selective nature
221 of our manipulation; while spine density decreased as we predicted at 2 and 4 weeks, neurons were able to
222 adapt by producing more spines because we did not alter synaptic architecture proteins that are implicated in
223 spine loss in schizophrenia, such as Cdc42 and Duo [60]. This would also explain why we observed an increase
224 in spine density at later time points, despite our initial prediction that loss of NMDARs would lead to a
225 reduction in synapse density due to activity-dependent disconnection [16]. Our findings indicate that NMDAR
226 ablation alone is not sufficient to induce long-lasting deficits in spine density, and suggests that other risk
227 factors for the disease – whether genetic or environmental – could also play a role in the failure to recover
228 from loss of neuropil observed in patients with schizophrenia.

229 We examined whether the changes in spine density were associated with functional consequences at
230 the synaptic level, and observed a significant increase in mEPSC frequency at 6 weeks. There were no
231 compensatory change in presynaptic glutamate release or AMPAR subunit composition, indicating that the
232 mEPSC frequency increase was primarily driven by the alterations in basilar spine density. Interestingly, we
233 also observed an increase in inhibitory signaling, with mIPSC amplitude significantly greater in the Grin1
234 group at 6 weeks. It was surprising that there were no mEPSC changes observed at 2 weeks, given the
235 significant reduction in basilar spine density at this early time point. This may be attributed to the fact that
236 early spine loss was primarily due to a reduction in weaker, less stable spines such as thin spines and filopodia,
237 which may make a smaller contribution to detectable levels of excitatory synaptic transmission [52]. In
238 contrast, mushroom spine density has a much smaller decrease in Grin1 mice at 2 weeks. At 6 weeks, the
239 density of mushroom spines, which are more stable and associated with stronger synapses [61], is equivalent
240 in the Grin1 and control groups and the density of weaker spines is significantly greater, which may be
241 sufficient to produce the observed increase in mEPSC frequency. Overall, these results suggest that subtle

242 changes in synaptic architecture may precede functional consequences for the network, with initial loss of
243 immature spines leading to a compensatory increase in connectivity and neurotransmission at later time points.

244 A key question in the field is whether pyramidal neurons or interneurons are primarily affected by
245 NMDAR hypofunction. Abnormal glutamatergic postsynaptic proteins and excessive synaptic pruning in
246 excitatory neurons [62–65] may lead to a subsequent downregulation of feedback inhibition, as reflected by
247 decreased interneuron expression of the activity-dependent proteins glutamate decarboxylase 67 and
248 parvalbumin [62,66,67]. However, we found that direct manipulation of NMDAR function in pyramidal
249 neurons (using the CaMKII promoter) did not recapitulate the effects of pan-neuronal NMDAR ablation (using
250 the hSyn promoter). This suggests that network reorganization may either require simultaneous loss of
251 NMDAR function in both pyramidal neurons and inhibitory interneurons, or that loss of NMDAR function
252 from inhibitory interneurons may instigate network reorganization. Several lines of evidence are consistent
253 with the latter possibility. Patients with schizophrenia have lower GABA synthesis [68], and reduced
254 expression of interneuron neuropeptides and GABA-A receptor subunits [69]. Reduced GAD67 expression is
255 also sufficient to induce schizophrenia-related behavioral phenotypes and altered excitatory and inhibitory
256 synaptic transmission [70,71]. In addition, interneurons are preferentially targeted by NMDAR antagonists
257 due to their more depolarized membrane potential [72], raising the question of whether previous studies using
258 NMDAR antagonism as a model for schizophrenia have exerted greater effects upon inhibitory neurons than
259 excitatory neurons. These issues can be addressed in future research using genetic manipulations developed to
260 target interneurons [73–77].

261 In addition to future studies targeting more specific cell types, our genome editing platform can be
262 readily adapted to manipulate expression of other genes strongly associated with schizophrenia, simply by
263 changing the viral vector gRNA sequence. These could include the Grin2a gene that encodes the GluN2A
264 subunit of NMDARs, or the Gria3 gene that encodes the GluA3 subunit of AMPA receptors [78]. While

265 schizophrenia is unlikely to involve complete loss of NMDAR function (e.g., our 6 week timepoint), the partial
266 loss of NMDAR function we observe at earlier timepoints may have greater translational relevance. The
267 progressive nature of our manipulation is thus valuable for correlating degree of NMDAR disruption with
268 network reorganization and behavioral output across time. In a parallel study, we have used this strategy to
269 track cognitive impairments produced by mPFC NMDAR ablation in a restless bandit task [79]. These
270 cognitive impairments develop within two weeks, and recover partially but not fully over time. Behavioral
271 deficits may persist because upregulation of AMPAR function cannot fully restore network operations
272 normally mediated by the unique biophysical properties of NMDARs, such as persistent neuronal firing during
273 working memory [80].

274 Our data address questions regarding the emergence of compensatory synaptic mechanisms, which are
275 central to developing our understanding of schizophrenia. Symptom onset may be triggered in patients by the
276 interaction of multiple layered risk factors [81]. One theory of the disease is that genetic mutations affecting
277 synapse formation and maintenance cause latent defects in cortical connectivity that are masked by the
278 hyperconnected state of the brain in early development, but as extraneous synapses are pruned during
279 adolescence, these vulnerabilities are laid bare and symptoms begin to occur in patients [38] In our model, the
280 cellular mechanisms of spine formation and maintenance were unchanged, and therefore early synaptic defects
281 could be compensated for by the production of additional immature spines. Although disruptions to the Grin1
282 gene alone cannot fully recapitulate the pathophysiology of schizophrenia, studying the effects of an isolated
283 Grin1 manipulation may help us understand why first-degree relatives of patients who have Grin1 mutations
284 but no additional genetic risk factors do not develop schizophrenia, or why patients with fewer biological or
285 environmental risk factors are able to successfully recover from first-episode psychosis. In contrast, other
286 patients may have altered gene expression related to neuronal survival [82] and architecture, such as
287 complement-mediated synaptic pruning [64,83], thus limiting the brain's ability to adapt to insults and leading
288 to more severe or long-lasting symptoms. Further study will be needed to examine how synaptic changes such

289 as NMDAR ablation interact with other risk factors to influence processes of synaptic dysfunction and
290 compensation relevant to schizophrenia. However, the preclinical success of newly developed therapies to treat
291 NMDAR hypofunction is an encouraging sign that these synaptic deficits and associated cognitive symptoms
292 may be able to be restored in patients [84].

ACKNOWLEDGEMENTS

Viral vectors used in this study were generated by the University of Minnesota Viral Innovation Core and the Center for Neural Circuits in Addiction (P30 DA048742). We thank the University of Minnesota University Imaging Core (SCR_020997) for the use of their facilities to conduct confocal imaging and analysis of dendritic spines, and Dr. Matthew Hearing for advice regarding electrophysiology experiments.

AUTHOR CONTRIBUTIONS

RMD, NMG, and PER were responsible for study design. RMD, APA, and CRQ conducted and analyzed electrophysiology recordings. RMD performed immunohistochemistry protocols. RMD and HA performed intracranial injections of viral vectors generated by EMFV. RMD, LBC, ATP, HA, and JSM conducted confocal imaging and analysis of dendritic spines. RMD and PER wrote the original draft of the manuscript, which all authors reviewed and edited before submission.

FUNDING

This work was supported by grants from the National Institutes of Health (T32MH115886 and F31MH133285 to RMD; T32GM008244, T32DA007234, and F30 DA060027 to APA; P50MH119569 to NHG and PER); the Howard Hughes Medical Institute (GT17865 to CRQ); the University of Minnesota's MnDRIVE (Minnesota's Discovery, Research, and Innovation Economy) initiative (PER); the University of Minnesota Life Sciences Summer Undergraduate Research Program (ATP); and the University of Minnesota Undergraduate Career Opportunities in Neuroscience and Undergraduate Research Opportunities Program (HA).

COMPETING INTERESTS

The authors declare no competing interests.

DATA AVAILABILITY STATEMENT

Data are available from the corresponding author upon request.

REFERENCES

1. Moghaddam B, Javitt D. From revolution to evolution: The glutamate hypothesis of schizophrenia and its implication for treatment. Neuropsychopharmacology. 2012;37:4–15.

2. Timms AE, Dorschner MO, Wechsler J, Choi KY, Kirkwood R, Girirajan S, et al. Support for the N-Methyl-D-Aspartate Receptor Hypofunction Hypothesis of Schizophrenia From Exome Sequencing in Multiplex Families. JAMA Psychiatry. 2013;70:582–590.

3. Ohi K, Hashimoto R, Ikeda M, Yamamori H, Yasuda Y, Fujimoto M, et al. Glutamate Networks Implicate Cognitive Impairments in Schizophrenia: Genome-Wide Association Studies of 52 Cognitive Phenotypes. Schizophr Bull. 2015;41:909–918.

4. Beneyto M, Meador-Woodruff JH. Lamina-specific abnormalities of NMDA receptor-associated postsynaptic protein transcripts in the prefrontal cortex in schizophrenia and bipolar disorder. Neuropsychopharmacology. 2008;33:2175–2186.

5. Catts VS, Lai YL, Weickert CS, Weickert TW, Catts S V. A quantitative review of the postmortem evidence for decreased cortical N-methyl-d-aspartate receptor expression levels in schizophrenia: How can we link molecular abnormalities to mismatch negativity deficits? Biol Psychol. 2016;116:57–67.

6. Poels EMP, Kegeles LS, Kantrowitz JT, Slifstein M, Javitt DC, Lieberman JA, et al. Imaging glutamate in schizophrenia: Review of findings and implications for drug discovery. Mol Psychiatry. 2014;19:20–29.

7. Bustillo JR, Upston J, Mayer EG, Jones T, Maudsley AA, Gasparovic C, et al. Glutamatergic hypo-function in the left superior and middle temporal gyri in early schizophrenia: a data-driven three-dimensional proton spectroscopic imaging study. Neuropsychopharmacology. 2020;45:1851–1859.

8. Javitt DC, Zukin RS. Recent advances in the phencyclidine model of schizophrenia. American Journal of Psychiatry. 1991;148:1301–1308.

9. Umbricht D, Schmid L, Koller R, Vollenweider FX, Hell D, Javitt DC. Ketamine-Induced Deficits in Auditory and Visual Context-Dependent Processing in Healthy Volunteers: Implications for Models of Cognitive Deficits in Schizophrenia. Arch Gen Psychiatry. 2000;57:1139–1147.

10. Lahti AC, Koffel B, Laporte D, Tamminga CA. Subanesthetic doses of ketamine stimulate psychosis in schizophrenia. Neuropsychopharmacology. 1995;13:9–19.

11. Malhotra AK, Pinals DA, Adler CM, Elman I, Clifton A, Pickar D, et al. Ketamine-induced exacerbation of psychotic symptoms and cognitive impairment in neuroleptic-free schizophrenics. Neuropsychopharmacology. 1997;17:141–150.

12. Lahti AC, Weiler MA, Michaelidis T, Parwani A, Tamminga CA. Effects of ketamine in normal and schizophrenic volunteers. Neuropsychopharmacology. 2001;25:455–467.

13. Jentsch JD, Tran A, Le D, Youngren KD, Roth RH. Reduces Mesoprefrontal Dopamine Utilization and Impairs Prefrontal Cortical-Dependent Cognition in the Rat. 1997;17:92–99.

14. Wang M, Yang Y, Wang C-J, Gamo NJ, Jin LE, Mazer JA, et al. NMDA receptors subserve persistent neuronal firing during working memory in dorsolateral prefrontal cortex. Neuron. 2013;77:736–749.

15. Blackman RK, Macdonald AW 3rd, Chafee MV. Effects of ketamine on context-processing performance in monkeys: a new animal model of cognitive deficits in schizophrenia. Neuropsychopharmacology. 2013;38:2090–2100.

16. Zick JL, Blackman RK, Crowe DA, Amirikian B, DeNicola AL, Netoff TI, et al. Blocking NMDAR Disrupts Spike Timing and Decouples Monkey Prefrontal Circuits: Implications for Activity-Dependent Disconnection in Schizophrenia. Neuron. 2018;98:1243-1255.e5.

17. Vinnakota C, Hudson MR, Ikeda K, Ide S, Mishina M, Sundram S, et al. Effects of NMDA receptor antagonists on working memory and gamma oscillations, and the mediating role of the GluN2D subunit. Neuropsychopharmacology. 2025:1–11.

18. Glantz LA, Lewis DA. Decreased dendritic spine density on prefrontal cortical pyramidal neurons in schizophrenia. Arch Gen Psychiatry. 2000;57:65–73.

19. Lewis DA, González-Burgos G. Neuroplasticity of neocortical circuits in schizophrenia. Neuropsychopharmacology. 2008;33:141–165.

20. Friston KJ. The disconnection hypothesis. Schizophr Res. 1998;30:115–125.

21. Stephan KE, Friston KJ, Frith CD. Dysconnection in schizophrenia: from abnormal synaptic plasticity to failures of self-monitoring. Schizophr Bull. 2009;35:509–527.

22. Zick JL, Blackman RK, Crowe DA, Amirikian B, DeNicola AL, Netoff TI, et al. Blocking NMDAR Disrupts Spike Timing and Decouples Monkey Prefrontal Circuits: Implications for Activity-Dependent Disconnection in Schizophrenia. Neuron. 2018;98:1243-1255.e5.

23. Zick JL, Crowe DA, Blackman RK, Schultz K, Bergstrand DW, DeNicola AL, et al. Disparate insults relevant to schizophrenia converge on impaired spike synchrony and weaker synaptic interactions in prefrontal local circuits. Current Biology. 2022;32:14-25.e4.

24. Eryilmaz H, Tanner AS, Ho NF, Nitenson AZ, Silverstein NJ, Petruzzi LJ, et al. Disrupted Working Memory Circuitry in Schizophrenia: Disentangling fMRI Markers of Core Pathology vs Other Aspects of Impaired Performance. Neuropsychopharmacology. 2016;41:2411–2420.

25. Hansen KB, Wollmuth LP, Bowie D, Furukawa H, Menniti FS, Sobolevsky AI, et al. Structure, Function, and Pharmacology of Glutamate Receptor Ion Channels. Pharmacol Rev. 2021;73:298–487.

26. Schüler T, Mesic I, Madry C, Bartholomäus I, Laube B. Formation of NR1/NR2 and NR1/NR3 heterodimers constitutes the initial step in N-methyl-D-aspartate receptor assembly. J Biol Chem. 2008;283:37–46.

27. Forrest D, Yuzaki M, Soares HD, Ng L, Luk DC, Sheng M, et al. Targeted disruption of NMDA receptor 1 gene abolishes NMDA response and results in neonatal death. Neuron. 1994;13:325–338.

28. Ramsey AJ, Milenkovic M, Oliveira AF, Escobedo-Lozoya Y, Seshadri S, Salahpour A, et al. Impaired NMDA receptor transmission alters striatal synapses and DISC1 protein in an age-dependent manner. Proc Natl Acad Sci U S A. 2011;108:5795–5800.

29. Alvarez VA, Ridenour DA, Sabatini BL. Distinct Structural and Ionotropic Roles of NMDA Receptors in Controlling Spine and Synapse Stability. The Journal of Neuroscience. 2007;27:7365 LP – 7376.

30. Datwani A, Iwasato T, Itohara S, Erzurumlu RS. NMDA receptor-dependent pattern transfer from afferents to postsynaptic cells and dendritic differentiation in the barrel cortex. Mol Cell Neurosci. 2002;21:477–492.

31. Ultanir SK, Kim JE, Hall BJ, Deerinck T, Ellisman M, Ghosh A. Regulation of spine morphology and spine density by NMDA receptor signaling in vivo. Proc Natl Acad Sci U S A. 2007;104:19553–19558.

32. Adesnik H, Li G, During MJ, Pleasure SJ, Nicoll RA. NMDA receptors inhibit synapse unsilencing during brain development. Proceedings of the National Academy of Sciences. 2008;105:5597–5602.

33. Venkatesan S, Binko MA, Mielnik CA, Ramsey AJ, Lambe EK. Deficits in integrative NMDA receptors caused by Grin1 disruption can be rescued in adulthood. Neuropsychopharmacology. 2023;48:1742–1751.

34. Selemon LD. A role for synaptic plasticity in the adolescent development of executive function. Transl Psychiatry. 2013;3:e238–e238.

35. Feinberg I. Schizophrenia: caused by a fault in programmed synaptic elimination during adolescence? J Psychiatr Res;17:319–334.

36. Weinberger DR. Implications of Normal Brain Development for the Pathogenesis of Schizophrenia. Arch Gen Psychiatry. 1987;44:660–669.

37. Lewis DA. Development of the Prefrontal Cortex during Adolescence: Insights into Vulnerable Neural Circuits in Schizophrenia. Neuropsychopharmacology. 1997;16:385–398.

38. Chafee MV, Averbeck BB. Unmasking Schizophrenia: Synaptic Pruning in Adolescence Reveals a Latent Physiological Vulnerability in Prefrontal Recurrent Networks. Biol Psychiatry. 2022;92:436–439.

39. Goodpaster CM, Christensen CR, Alturki MB, DeNardo LA. Prefrontal cortex development and its implications in mental illness. Neuropsychopharmacology. 2025:1–15.

40. Florance NR, Davis RL, Lam C, Szperka C, Zhou L, Ahmad S, et al. Anti-N-methyl-D-aspartate receptor (NMDAR) encephalitis in children and adolescents. Ann Neurol. 2009;66:11–18.

41. Kayser MS, Dalmau J. Anti-NMDA receptor encephalitis, autoimmunity, and psychosis. Schizophr Res. 2016;176:36–40.

42. Straub C, Granger AJ, Saulnier JL, Sabatini BL. CRISPR/Cas9-Mediated Gene Knock-Down in Post-Mitotic Neurons. PLoS One. 2014;9:e105584.

43. Incontro S, Asensio CS, Edwards RH, Nicoll RA. Efficient, complete deletion of synaptic proteins using CRISPR. Neuron. 2014;83:1051–1057.

44. Platt RJ, Chen S, Zhou Y, Yim MJ, Swiech L, Kempton HR, et al. CRISPR-Cas9 knockin mice for genome editing and cancer modeling. Cell. 2014;159:440–455.

45. Brandner DD, Retzlaff CL, Kocharian A, Stieve BJ, Mashal MA, Mermelstein PG, et al. Neuroligin-3 in dopaminergic circuits promotes behavioural and neurobiological adaptations to chronic morphine exposure. Addiction Biology. 2023;28:e13247.

46. Anderson EM, Demis S, Wrucke B, Engelhardt A, Hearing MC. Infralimbic cortex pyramidal neuron GIRK signaling contributes to regulation of cognitive flexibility but not affect-related behavior in male mice. Physiol Behav. 2021;242:113597.

47. Hunker AC, Soden ME, Krayushkina D, Heymann G, Awatramani R, Zweifel LS. Conditional Single Vector CRISPR/SaCas9 Viruses for Efficient Mutagenesis in the Adult Mouse Nervous System. Cell Rep. 2020;30:4303-4316.e6.

48. Huttenlocher PR. Synaptic density in human frontal cortex — Developmental changes and effects of aging. Brain Res. 1979;163:195–205.

49. Huttenlocher PR, Dabholkar AS. Regional differences in synaptogenesis in human cerebral cortex. Journal of Comparative Neurology. 1997;387:167–178.

50. Musket CW, Kuo SS, Rupert PE, Almasy L, Gur RC, Prasad K, et al. Why does age of onset predict clinical severity in schizophrenia? A multiplex extended pedigree study. American Journal of Medical Genetics Part B: Neuropsychiatric Genetics. 2020;183:403–411.

51. Rothwell PE, Hayton SJ, Sun GL, Fuccillo MV., Kook Lim B, Malenka RC. Input- and Output-Specific Regulation of Serial Order Performance by Corticostriatal Circuits. Neuron. 2015;88:345–356.

52. Arellano JI, Benavides-Piccione R, Defelipe J, Yuste R. Ultrastructure of dendritic spines: correlation between synaptic and spine morphologies. Front Neurosci. 2007;1:131–143.

53. Williams SR, Stuart GJ. Dependence of EPSP efficacy on synapse location in neocortical pyramidal neurons. Science. 2002;295:1907–1910.

54. Hume RI, Dingledine R, Heinemann SF. Identification of a site in glutamate receptor subunits that controls calcium permeability. Science. 1991;253:1028–1031.

55. Liu SQ, Cull-Candy SG. Synaptic activity at calcium-permeable AMPA receptors induces a switch in receptor subtype. Nature. 2000;405:454–458.

56. Bourne J, Harris KM. Do thin spines learn to be mushroom spines that remember? Curr Opin Neurobiol. 2007;17:381–386.

57. MacDonald ML, Alhassan J, Newman JT, Richard M, Gu H, Kelly RM, et al. Selective Loss of Smaller Spines in Schizophrenia. Am J Psychiatry. 2017;174:586–594.

58. McKinney BC, MacDonald ML, Newman JT, Shelton MA, DeGiosio RA, Kelly RM, et al. Density of small dendritic spines and microtubule-associated-protein-2 immunoreactivity in the primary auditory cortex of subjects with schizophrenia. Neuropsychopharmacology. 2019;44:1055–1061.

59. Spruston N. Pyramidal neurons: Dendritic structure and synaptic integration. Nat Rev Neurosci. 2008;9:206–221.

60. Hill JJ, Hashimoto T, Lewis DA. Molecular mechanisms contributing to dendritic spine alterations in the prefrontal cortex of subjects with schizophrenia. Mol Psychiatry. 2006;11:557–566.

61. Matsuzaki M, Ellis-Davies GCR, Nemoto T, Miyashita Y, Iino M, Kasai H. Dendritic spine geometry is critical for AMPA receptor expression in hippocampal CA1 pyramidal neurons. Nat Neurosci. 2001;4:1086–1092.

62. Lewis DA, Curley AA, Glausier JR, Volk DW. Cortical parvalbumin interneurons and cognitive dysfunction in schizophrenia. Trends Neurosci. 2012;35:57–67.

63. Fromer M, Pocklington AJ, Kavanagh DH, Williams HJ, Dwyer S, Gormley P, et al. De novo mutations in schizophrenia implicate synaptic networks. Nature. 2014;506:179–184.

64. Sekar A, Bialas AR, de Rivera H, Davis A, Hammond TR, Kamitaki N, et al. Schizophrenia risk from complex variation of complement component 4. Nature. 2016;530:177–183.

65. Consortium SWG of the PG. Biological insights from 108 schizophrenia-associated genetic loci. Nature. 2014;511:421–427.

66. Hashimoto T, Volk DW, Eggan SM, Mirnics K, Pierri JN, Sun Z, et al. Gene expression deficits in a subclass of GABA neurons in the prefrontal cortex of subjects with schizophrenia. J Neurosci. 2003;23:6315–6326.

67. Enwright JF, Sanapala S, Foglio A, Berry R, Fish KN, Lewis DA. Reduced Labeling of Parvalbumin Neurons and Perineuronal Nets in the Dorsolateral Prefrontal Cortex of Subjects with Schizophrenia. Neuropsychopharmacology. 2016;41:2206–2214.

68. Ohnuma T, Augood SJ, Arai H, McKenna PJ, Emson PC. Measurement of GABAergic parameters in the prefrontal cortex in schizophrenia: focus on GABA content, GABAA receptor-1α subunit messenger RNA and human GABA transporter-1 (hGAT-1) messenger RNA expression. Neuroscience. 1999;93:441–448.

69. Hashimoto T, Arion D, Unger T, Maldonado-Avilés JG, Morris HM, Volk DW, et al. Alterations in GABA-related transcriptome in the dorsolateral prefrontal cortex of subjects with schizophrenia. Mol Psychiatry. 2008;13:147–161.

70. Fujihara K, Miwa H, Kakizaki T, Kaneko R, Mikuni M, Tanahira C, et al. Glutamate Decarboxylase 67 Deficiency in a Subset of GABAergic Neurons Induces Schizophrenia-Related Phenotypes. Neuropsychopharmacology. 2015;40:2475–2486.

71. Kolata SM, Nakao K, Jeevakumar V, Farmer-Alroth EL, Fujita Y, Bartley AF, et al. Neuropsychiatric Phenotypes Produced by GABA Reduction in Mouse Cortex and Hippocampus. Neuropsychopharmacology. 2018;43:1445–1456.

72. McCutcheon RA, Krystal JH, Howes OD. Dopamine and glutamate in schizophrenia: biology, symptoms and treatment. World Psychiatry. 2020;19:15–33.

73. Belforte JE, Zsiros V, Sklar ER, Jiang Z, Yu G, Li Y, et al. Postnatal NMDA receptor ablation in corticolimbic interneurons confers schizophrenia-like phenotypes. Nat Neurosci. 2010;13:76–83.

74. Korotkova T, Fuchs EC, Ponomarenko A, von Engelhardt J, Monyer H. NMDA receptor ablation on parvalbumin-positive interneurons impairs hippocampal synchrony, spatial representations, and working memory. Neuron. 2010;68:557–569.

75. Billingslea EN, Tatard-Leitman VM, Anguiano J, Jutzeler CR, Suh J, Saunders JA, et al. Parvalbumin Cell Ablation of NMDA-R1 Causes Increased Resting Network Excitability with Associated Social and Self-Care Deficits. Neuropsychopharmacology. 2014;39:1603–1613.

76. Jadi MP, Behrens MM, Sejnowski TJ. Abnormal Gamma Oscillations in N-Methyl-D-Aspartate Receptor Hypofunction Models of Schizophrenia. Biol Psychiatry. 2016;79:716–726.

77. Uehara JM, Gomez Acosta M, Bello EP, Belforte JE. Early postnatal NMDA receptor ablation in cortical interneurons impairs affective state discrimination and social functioning. Neuropsychopharmacology. 2025;50:1119–1129.

78. Singh T, Poterba T, Curtis D, Akil H, Al Eissa M, Barchas JD, et al. Rare coding variants in ten genes confer substantial risk for schizophrenia. Nature. 2022;604:509–516.

79. Knep E, Velosa A, Mueller D, Chen CS, Vinogradov S, Chafee M, et al. NMDA receptor ablation in medial prefrontal cortex disrupts value updating and reward history integration. BioRxiv. 2025. 10 December 2025. https://doi.org/10.64898/2025.12.06.692679.

80. Wang M, Yang Y, Wang CJ, Gamo NJ, Jin LE, Mazer JA, et al. NMDA Receptors Subserve Persistent Neuronal Firing during Working Memory in Dorsolateral Prefrontal Cortex. Neuron. 2013;77:736–749.

81. Vinogradov S, Chafee MV, Lee E, Morishita H. Psychosis spectrum illnesses as disorders of prefrontal critical period plasticity. Neuropsychopharmacology. 2023;48:168–185.

82. Pandya CD, Kutiyanawalla A, Pillai A. BDNF-TrkB signaling and neuroprotection in schizophrenia. Asian J Psychiatr. 2013;6:22–28.

83. Gallego JA, Blanco EA, Morell C, Lencz T, Malhotra AK. Complement component C4 levels in the cerebrospinal fluid and plasma of patients with schizophrenia. Neuropsychopharmacology. 2021;46:1140–1144.

84. Oosterlaken M, Rogliardo A, Lipina T, Lafon P-A, Tsitokana ME, Keck M, et al. Nanobody therapy rescues behavioural deficits of NMDA receptor hypofunction. Nature. 2025. 2025. https://doi.org/10.1038/s41586-025-09265-8.

FIGURES and FIGURE LEGENDS

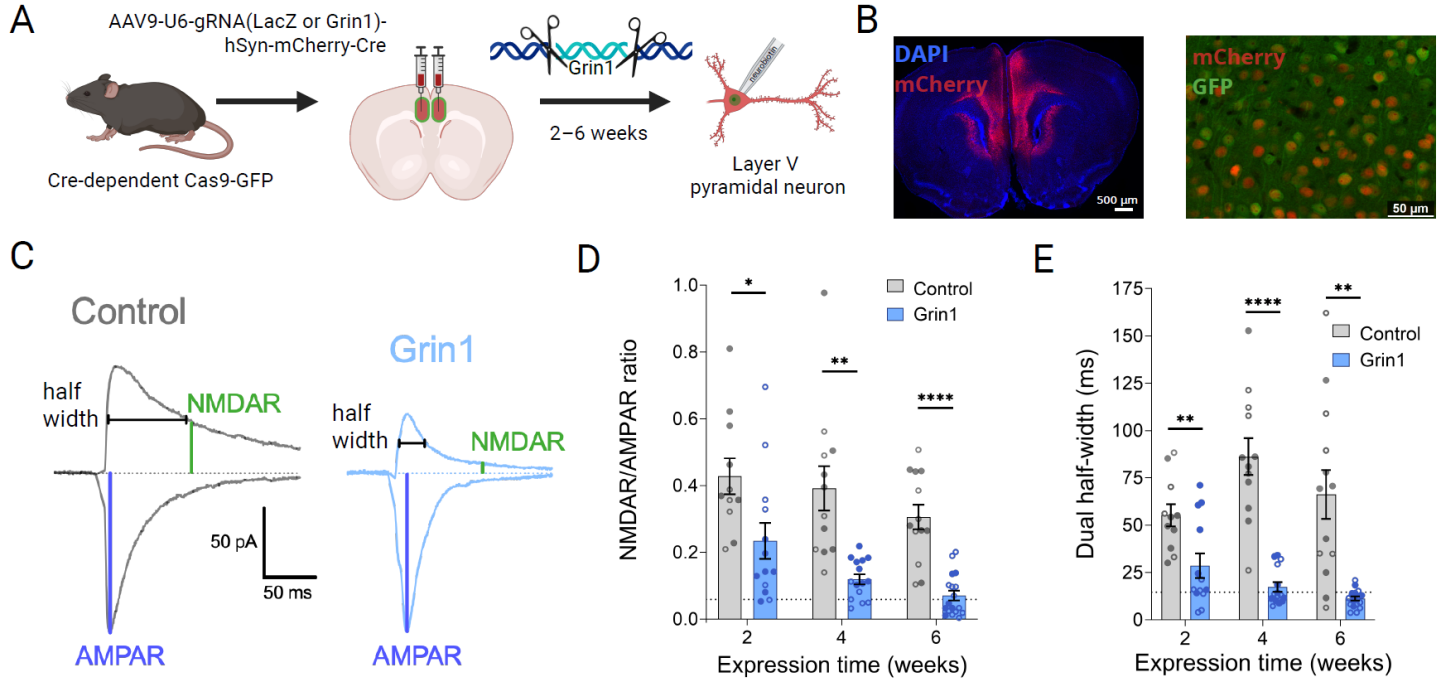

Figure 1. Grin1 ablation decreases NMDAR function. (A) Experimental overview showing mPFC intracranial injection of gRNA virus to ablate Grin1 gene expression, followed by whole-cell patch-clamp recording and neurobiotin cell filling. **(B)** mPFC expression of mCherry and GFP in virally transduced cells (left: 10x magnification tiled image, right: 20x magnification). **(C)** Sample traces of evoked excitatory postsynaptic currents (EPSCs) at -70 mV and +40 mV to measure AMPAR and NMDAR currents, respectively. **(D)** Grin1 ablation reduces NMDAR/AMPAR ratio with a significant main effect of virus ($F_{1,70} = 58.80$, $P < 0.0001$) (control n/N=11/4, 12/5, and 13/6 at 2, 4 and 6 weeks; Grin1 n/N=13/4, 15/6, and 18/6 at 2, 4 and 6 weeks) and **(E)** half-width of the dual component EPSC with a significant main effect of virus ($F_{1,70} = 74.74$, $P < 0.0001$) and time x virus interaction ($F_{2,70} = 3.670$, $P = 0.0305$) (same sample sizes as D). Dotted lines indicate values for NMDAR/AMPAR ratio (D) and dual half-width (E) measured under pharmacological blockade of NMDAR function with 50 µM D-APV (n=4). Data are mean ± s.e.m. for all panels; open and closed circles indicate recordings from female and male mice, respectively. *P < 0.05, **P < 0.01, ****P < 0.0001; three-way ANOVA followed by simple effect test; see Data S1 for complete statistics. https://BioRender.com/8iil7j5

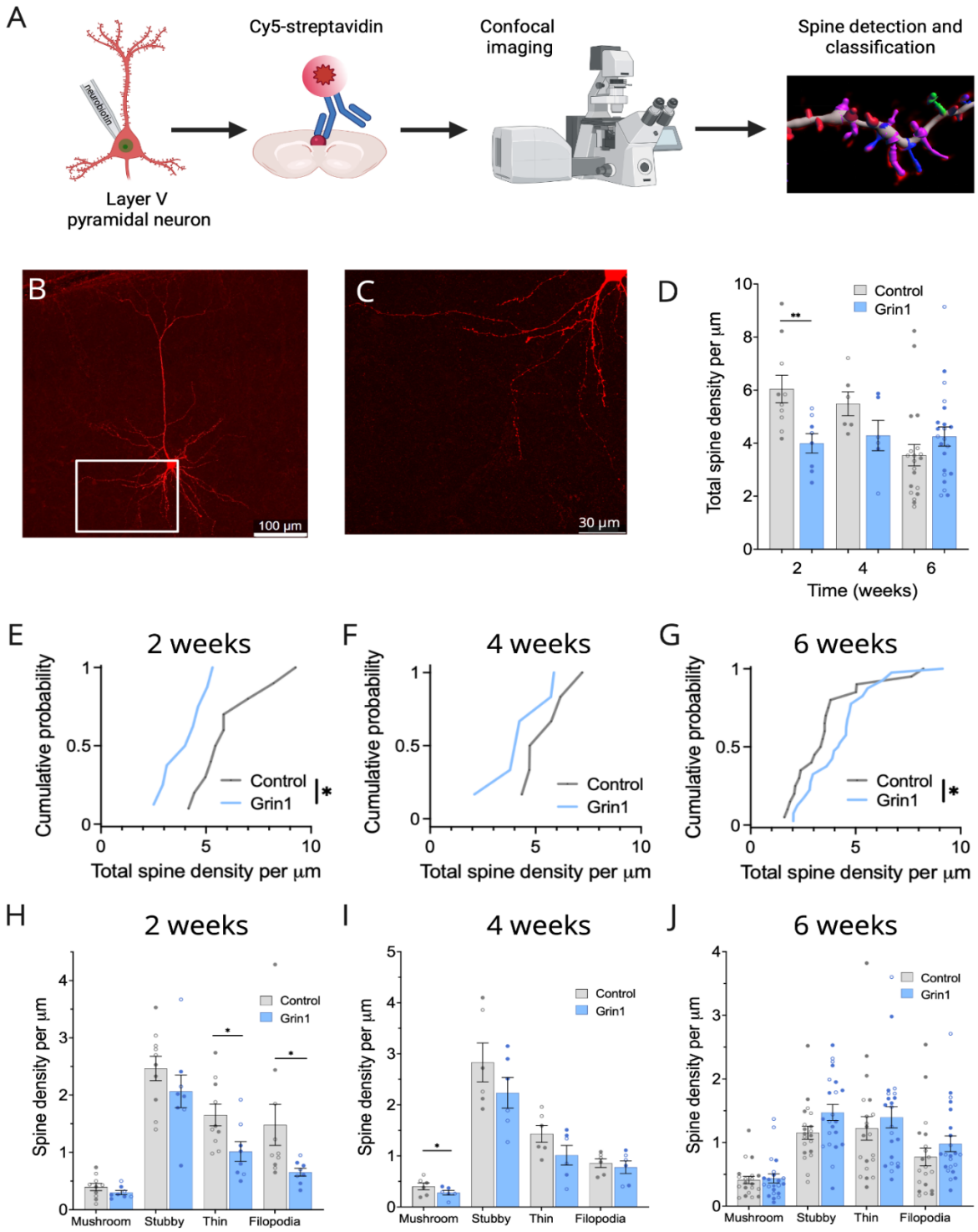

Figure 2. NMDAR ablation causes an initial decrease and subsequent increase in basilar spine density. (A) Schematic showing neurobiotin filling, imaging, and analysis of dendritic spines. **(B-C)** Sample image of the basilar dendrites of a layer V mPFC pyramidal neuron at 20x magnification (B) and 63x magnification (C). **(D)** Decrease in total basilar spine density in the Grin1 group at two weeks, with a trend towards increased density at six weeks (main effect of virus, $F_{1,60} = 4.709$, $P = 0.0340$; virus x time interaction, $F_{2,60} = 5.307$, P =

0.0075) (control n/N = 10/5, 6/4, and 20/12 at 2, 4 and 6 weeks; Grin1 n/N = 8/4, 6/4, and 22/8 at 2, 4 and 6 weeks). **(E, H)** Basilar spine density distribution is significantly reduced in the Grin1 group at two weeks (D = 0.6000, P = 0.0499), driven by significant reductions in thin spines ($F_{1,14}$ = 5.971, P = 0.0284) and filopodia ($F_{1,14}$ = 4.935, P = 0.0433). **(F, I)** Density of mushroom spines is significantly reduced at four weeks ($F_{1,8}$ = 6.689, P = 0.0323). **(G, J)** Basilar spine density distribution is significantly increased at six weeks (D = 0.4364, P = 0.0370), with a trend towards increased density in immature spine categories. Sample sizes for panels E-J are the same as panel D. Data are mean ± s.e.m. for all panels; open and closed circles indicate recordings from female and male mice, respectively. *P < 0.05, **P < 0.01; three-way ANOVA followed by simple effect test (D); Kolmogorov-Smirnov test (E-G); or two-way ANOVA (H-J); see Data S1 for complete statistics. https://BioRender.com/46hxi18

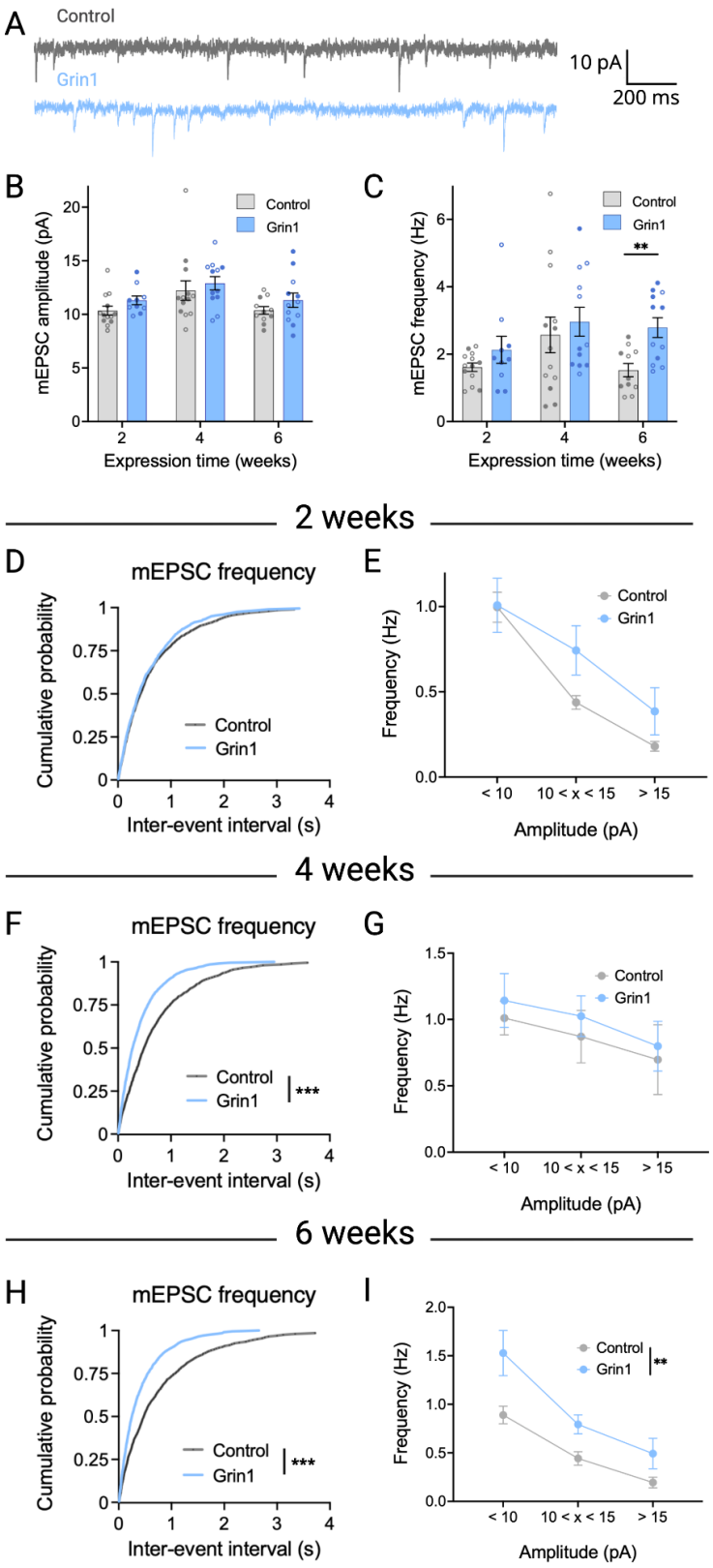

Figure 3. AMPAR-mediated synaptic transmission increases over time following NMDAR ablation. (A) Sample traces of miniature excitatory postsynaptic currents (mEPSCs) at 6 weeks. **(B)** No change in mEPSC amplitude at any time point (control n/N = 13/5, 13/6, and 11/5 at 2, 4 and 6 weeks; Grin1 n/N = 10/4, 12/4, and

12/6 at 2, 4 and 6 weeks). **(C)** mEPSC frequency is significantly increased at six weeks (main effect of virus: $F_{1,59} = 6.063$, $P = 0.0167$). **(D-E)** No change in the distribution of mEPSC frequency across all event sizes at two weeks. **(F)** There is a significant leftward shift in the distribution of mEPSC inter-event interval in the Grin1 group at four weeks ($D = 0.2100$, $P = 0.0003$) and **(H)** six weeks ($D = 0.2150$, $P = 0.0002$), with a similar effect across event amplitudes (main effect of virus at six weeks, $F_{1,21} = 12.12$, $P = 0.0022$) **(G, I).** Sample sizes for panels C-I are the same as panel B. Data are mean ± s.e.m. for all panels; open and closed circles indicate recordings from female and male mice, respectively. **$P < 0.01$, ***$P < 0.001$; three-way ANOVA followed by simple effect test (B-C); Kolmogorov-Smirnov test (D, F, H); or two-way ANOVA (E, G, I); see Data S1 for complete statistics. https://BioRender.com/iazf88r

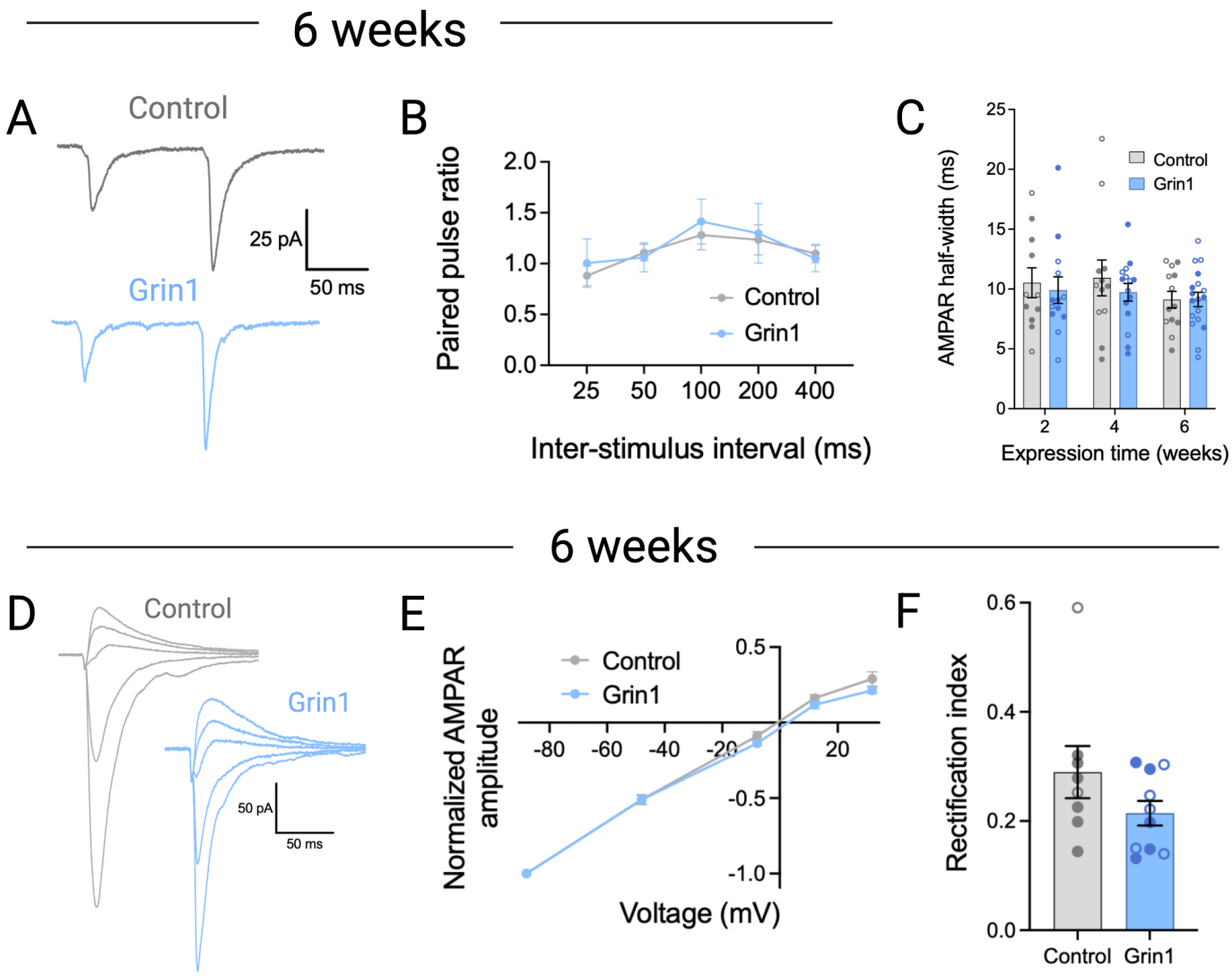

Figure 4. Paired-pulse ratio and AMPAR input-output properties are unchanged after NMDAR ablation. **(A)** Sample traces of EPSCs evoked in response to paired pulse stimulation after 6 weeks of virus expression. **(B)** No significant difference in paired pulse ratio (control n/N = 13-15/7; Grin1 n/N = 11-14/8). **(C)** Half width of the AMPA EPSC is unchanged at all time points (control n/N = 11/4, 12/5, and 13/6 at 2, 4 and 6 weeks; Grin1 n/N = 13/4, 15/6, and 18/6 at 2, 4 and 6 weeks). **(D)** Sample traces of AMPAR EPSCs evoked at different voltages. **(E)** AMPA current-voltage plot shows no significant difference between groups (control n/N = 6-12/7; Grin1 n/N = 3-13/7). **(F)** The rectification index is not significantly different between groups (control n/N = 8/4; Grin1 n/N = 10/7). Data are mean ± s.e.m. for all panels; open and closed circles indicate recordings from female and male mice, respectively. Mixed-effects analysis (B, E); three-way ANOVA (C); or Welch's two-tailed t test (F); see Data S1 for complete statistics. https://BioRender.com/mlt9v8e

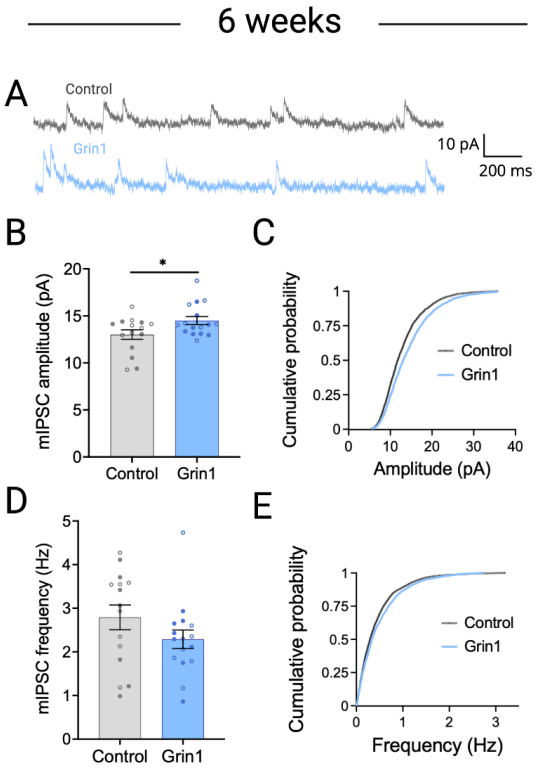

F

Experimental measure	2 weeks	4 weeks	6 weeks
NMDAR/AMPAR ratio	↓	↓	↓
Basilar spine density	↓	↓	↑
mEPSC frequency	–	–	↑
mIPSC amplitude			↑

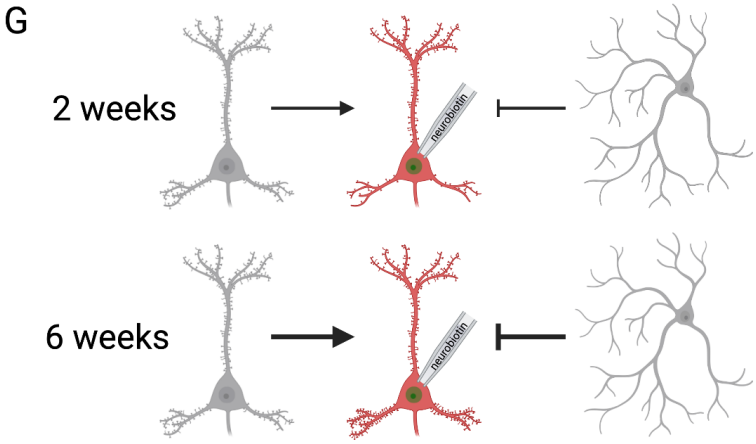

Figure 5. Inhibitory synaptic input to pyramidal neurons is increased after NMDAR ablation. (A) Sample traces of miniature inhibitory postsynaptic currents (mIPSCs) after 6 weeks of virus expression. **(B-C)** mIPSC amplitude is significantly increased in the Grin1 group (main effect of virus, $F_{1,27} = 5.350$, $P = 0.0286$), with no change in the cumulative probability distribution**. (D-E)** mIPSC amplitude is unchanged following NMDAR ablation (for B-E: control n/N = 15/5; Grin1 n/N = 16/4). Data are mean ± s.e.m. for all panels; open and closed circles indicate recordings from female and male mice, respectively. *P <0.05; two-way ANOVA (B, D); or Kolmogorov-Smirnov test (C, E); see Data S1 for complete statistics. **(F)** Summary table and figure **(G)** illustrating functional and structural changes over time following NMDAR ablation. https://BioRender.com/ilmaze5